



Late Holocene Orbital Forcing and Solar Activity on the Kuroshio Current of Subtropical North Pacific at Different Timescales

Xue Ding^{1,2}, Bangqi Hu^{1,2*}, Jun Li³, Jingtao Zhao^{1,2}, Yue Yao⁴, Qing Li^{1,2}, Jianghu Lan^{5,6}, Xufeng Zheng⁷ and Liang Yi⁸

¹Qingdao Institute of Marine Geology, Qingdao, China, ²Laboratory for Marine Mineral Resources, Pilot National Laboratory for Marine Science and Technology, Qingdao, China, ³Wuhan Geological Survey Center, Wuhan, China, ⁴Institute of Marine Science and Technology, Shandong University, Qingdao, China, ⁵State Key Laboratory of Loess and Quaternary Geology, Institute of Earth Environment, Chinese Academy of Sciences, Xi'an, China, ⁶Center for Excellence in Quaternary Science and Global Change, Chinese Academy of Sciences, Xi'an, China, ⁷State Key Laboratory of Marine Resource Utilization in South China Sea, Hainan University, Haikou, China, ⁸State Key Laboratory of Marine Geology, Tongji University, Shanghai, China

OPEN ACCESS

Edited by:

Xiting Liu,
Ocean University of China, China

Reviewed by:

Liang Dong,
Shanghai Jiao Tong University, China
Zhaokai Xu,
Institute of Oceanology (CAS), China

*Correspondence:

Bangqi Hu
bangqihu@gmail.com

Specialty section:

This article was submitted to
"Marine Geoscience",
a section of the journal
Frontiers in Earth Science

Received: 29 December 2021

Accepted: 31 January 2022

Published: 14 March 2022

Citation:

Ding X, Hu B, Li J, Zhao J, Yao Y, Li Q,
Lan J, Zheng X and Yi L (2022) Late
Holocene Orbital Forcing and Solar
Activity on the Kuroshio Current of
Subtropical North Pacific at
Different Timescales.
Front. Earth Sci. 10:845228.
doi: 10.3389/feart.2022.845228

The North Pacific subtropical gyre (NPSTG) redistributes heat and moisture between low and high latitudes and plays a key role in modulating the global climate change and ecosystem. Recent evidence suggests intensification and poleward shift of the subtropical gyres over the last decades due to global warming, but insufficient observations have hampered insight into the integrated effects of ocean-atmosphere interactions at longer timescales. Here we present the first high-resolution (~12 years) grain-size record from Core CF1 in the Okinawa Trough, western subtropical North Pacific, to reconstruct the evolution of the western boundary Kuroshio Current (KC) of NPSTG during the Late Holocene. Our results indicate the KC slow-down during 4.6–2.0 ka, followed by quick enhancement after 2.0 ka, with centennial-scale variabilities (500–700 years) superimposed on the long-term trend. Over millennial timescales, gradually increased pole-to-equator thermal gradient, due to orbital forcing mechanisms, resulted in long-term enhanced KC, whereas solar activity triggered phase changes in the tropical Pacific mean state and controlled KC anomalies on centennial timescales. We suggest that both forcing mechanisms resulted in ocean-atmosphere feedback provoking concurrent changes in mid-latitude westerly and subtropical easterly winds over the North Pacific, alternating their dominance as source regions causing the dynamic changes of KC at different timescales. Our findings offer insight into the role of external forcing mechanisms in the NPSTG changes before the Anthropocene, which have profound implications for the deeper understanding of changes in ocean gyres under global warming scenarios.

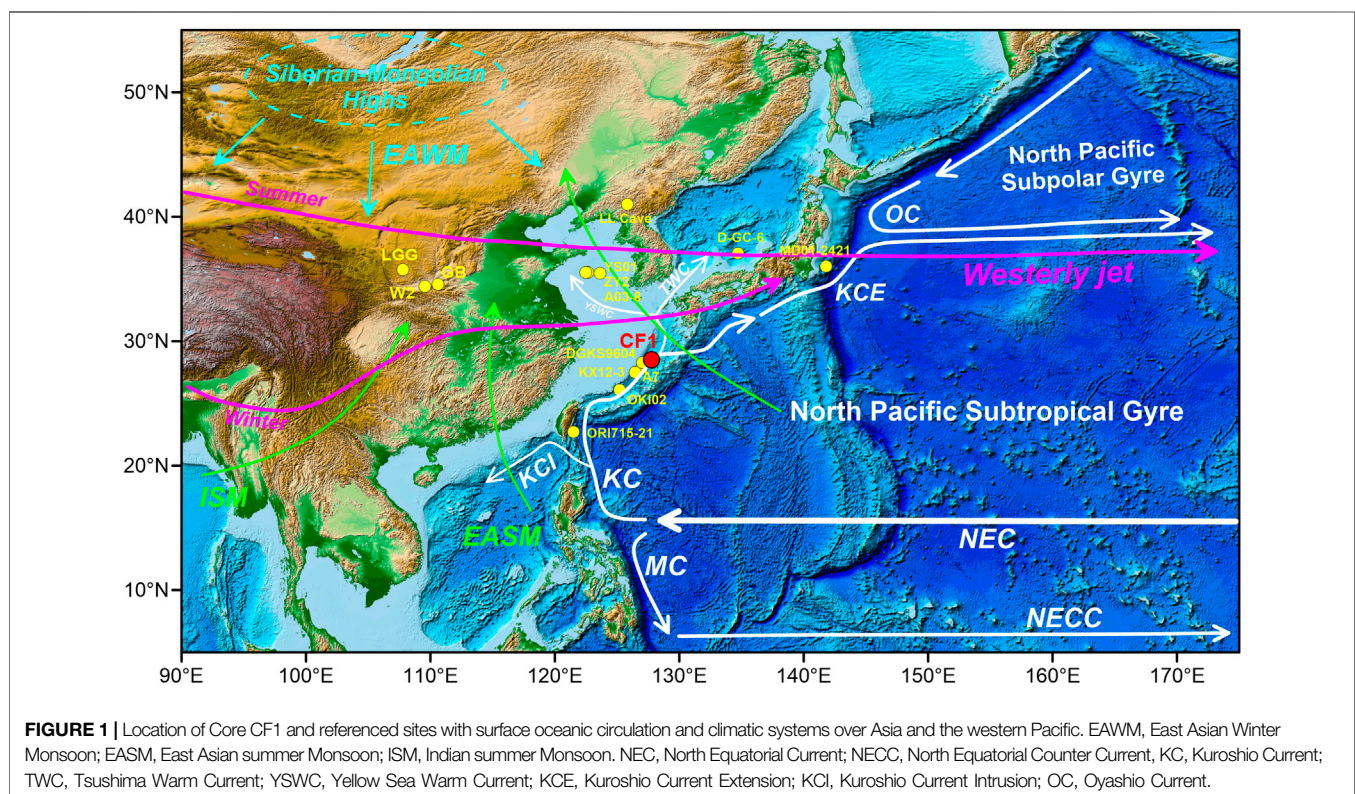
Keywords: Kuroshio Current, Okinawa Trough, solar forcing, ocean-atmosphere coupling, Late Holocene, westerly

INTRODUCTION

As one of strong wind-driven western boundary currents (WBCs) of the North Pacific Subtropical Gyre (NPSTG), the Kuroshio Current (KC) originates from the northward branch of the North Equatorial Current (NEC), enters the Okinawa Trough off northeastern Taiwan, and then flows along the continental slope of East China Sea (ECS) before turning eastward through the Tokara Strait (**Figure 1**). The KC transports substantial amounts of heat and moisture poleward and thus plays an essential role in global climate change and heat balance (Hu et al., 2015). Despite recent progress in understanding the seasonal and interannual variabilities of the KC, which are generally related to El-Niño–Southern Oscillation (ENSO), Pacific Decadal Oscillation (PDO), and East Asian monsoon systems, there is ongoing debate concerning the KC dynamics over longer time scales (Nakamura, 2020). For ENSO, during La Niña events, the zonal sea surface temperature (SST) gradient across the equatorial Pacific Ocean enhances, strengthening the Walker Circulation with the easterly wind prevails, and the NEC bifurcation latitude (NBL) occurs at its southernmost position, the transported volumes of the KC increases; and the opposite occurs during El Niño events (Hu et al., 2015). Previous studies demonstrated that the variability of the KC along the margin of the East China Sea at interdecadal scales is more closely with PDO than with ENSO, and the KC generally decelerated during negative PDO with enhanced trade winds and weakened westerlies, and vice versa (Andres et al., 2009; Wu, 2013; Wu

et al., 2019). Recently, the potential effects of global warming on the KC and other WBCs have raised significant concerns, suggesting that a stronger warming trend occurred over the KC during the past century, possibly associated with a synchronous poleward shift and/or intensification of WBCs (Wu et al., 2012; England et al., 2014; Hu et al., 2015; Yang et al., 2016; Yang et al., 2020). Reconstruction of the response of KC intensity to different forcing mechanisms at longer timescales will thus aid in better quantifying future changes in the WBCs.

Sedimentary records from the Okinawa Trough, under the influence of the KC, are ideally located to reveal the oceanic-atmospheric dynamic influences that originated in both the tropical and high latitudes of North Pacific (Jian et al., 2000; Zheng et al., 2014; Zheng et al., 2016; Lim et al., 2017; Jiang et al., 2019; Li et al., 2019; Li et al., 2020). Although many studies have illustrated changes in the KC intensity and its flow path since the last glacial maximum (LGM), the different forcing mechanisms driving these changes are still debated. Specifically, most available records are adequate for characterizing long-term trends of the KC, e.g., the Holocene, but do not capture the short-term climate oscillations, largely due to the scarcity of robust proxy and/or low resolution of climate archives (Yamazaki et al., 2016). Here, we present a well-dated and high-resolution grain-size record from the middle Okinawa Trough that documents the evolution of the KC intensity during the last 4.6 kyr. The aim of this study is to characterize the long-term trend and centennial periodicity of the KC during the Late Holocene and to discuss the forcing mechanisms that caused them.



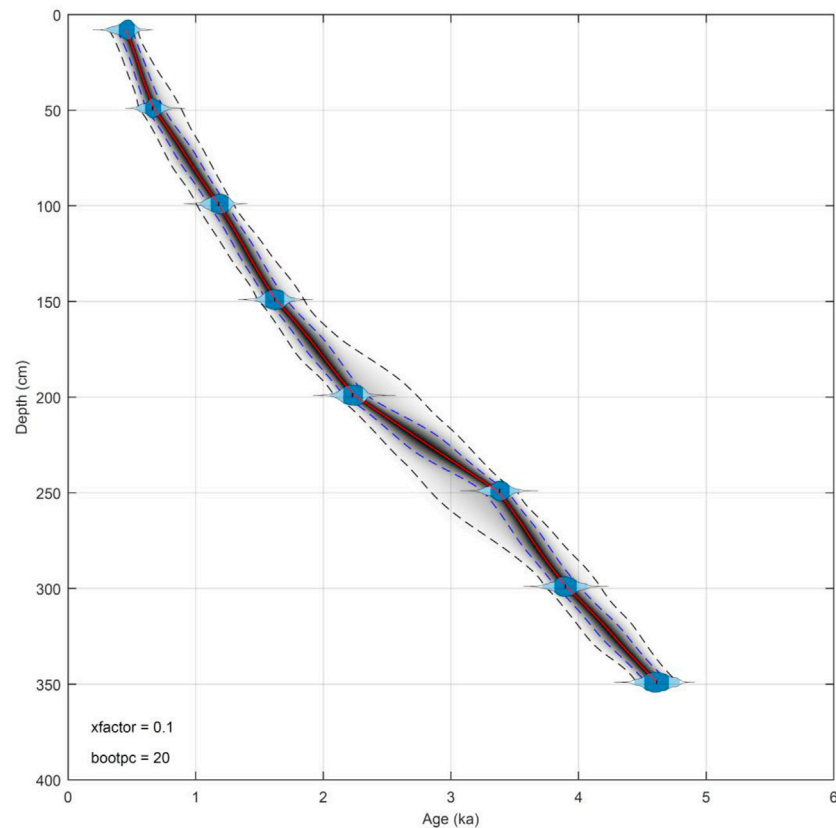


FIGURE 2 | Age model of Core CF1 using the recently published age-depth modeling routine “Undatable” (Lougheed and Obrochta, 2019). Age error estimates of nonnormally 68 and 95% percentiles are also shown.

TABLE 1 | Accelerator mass spectrometry (AMS) radiocarbon (^{14}C) dates of Core CF1 samples.

BETA No.	Samples	Depth/cm	Conventional Age \pm error/yr BP	2σ -Range/cal. yr BP	Median Probability/cal. yr BP
491946	CF1-1	8–10	1,040 \pm 30	302–565	456
491947	CF1-2	48–50	1,300 \pm 30	534–789	665
491948	CF1-3	98–100	1,810 \pm 30	1,032–1,305	1,181
491949	CF1-4	148–150	2,230 \pm 30	1,463–1,781	1,620
491950	CF1-5	198–200	2,730 \pm 30	2,056–2,377	2,231
491951	CF1-6	248–250	3,670 \pm 30	3,223–3,541	3,383
491952	CF1-7	298–300	4,080 \pm 30	3,717–4,075	3,898
491953	CF1-8	348–350	4,620 \pm 30	4,437–4,796	4,615

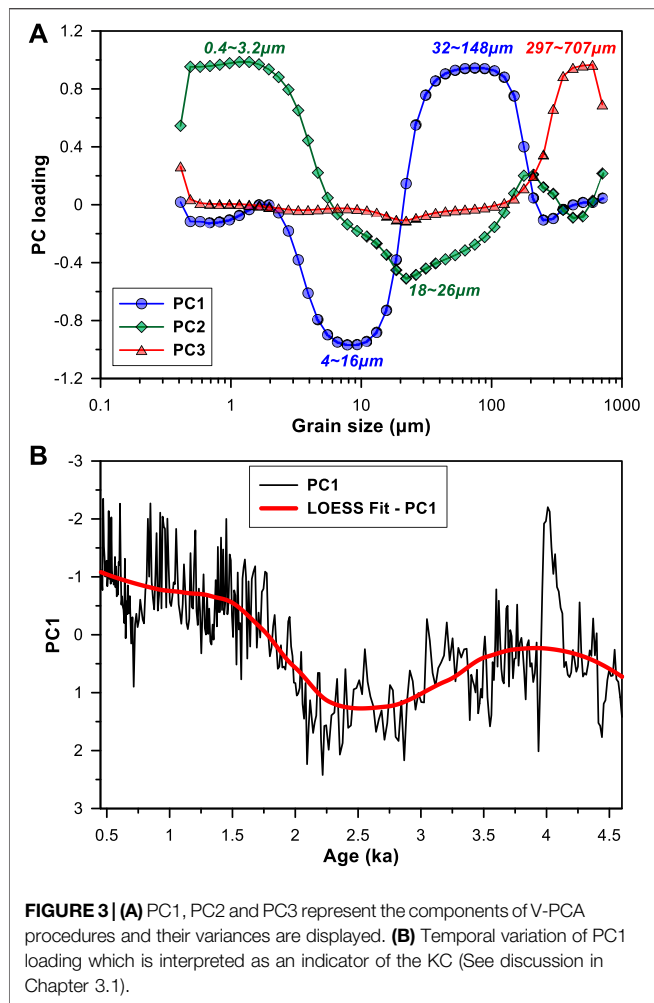
MATERIALS AND METHODS

Sediment Core and Chronology

Gravity Core CF1 (water depth 1,180 m; 127.43°E, 28.42°N) (Figure 1), with a length of 351 cm, was retrieved from the western slope of the middle Okinawa Trough during a cruise in 2012. The core was sliced into 1-cm-thick subsamples after the cruise. The lithology of Core CF1 consists of homogeneous gray silty clay. No obvious depositional hiatus or turbidite layers were found within Core CF1. The planktonic foraminiferal species *Neogloboquadrina dutertrei* from the $>150\ \mu\text{m}$ size fraction of eight layers were picked

up for accelerator mass spectrometry radiocarbon (AMS ^{14}C) dating at Beta Analytic Inc.(Florida, United States) (Figure 2).

Considering the top segment of Core CF1 was damaged and lost during the sampling process, the age model of Core CF1 between 8 and 348 cm (Figure 2A) was constructed using the recently published age-depth modeling routine “Undatable” (Lougheed and Obrochta, 2019). The deterministic routines of Undatable, with a positive sedimentation rate prior and bootstrapping, result in median and mean age-depth models with age error estimates of non-normally 68% and 95% percentiles (Lougheed and Obrochta, 2019). Here, the AMS ^{14}C ages were calibrated to a calendar age



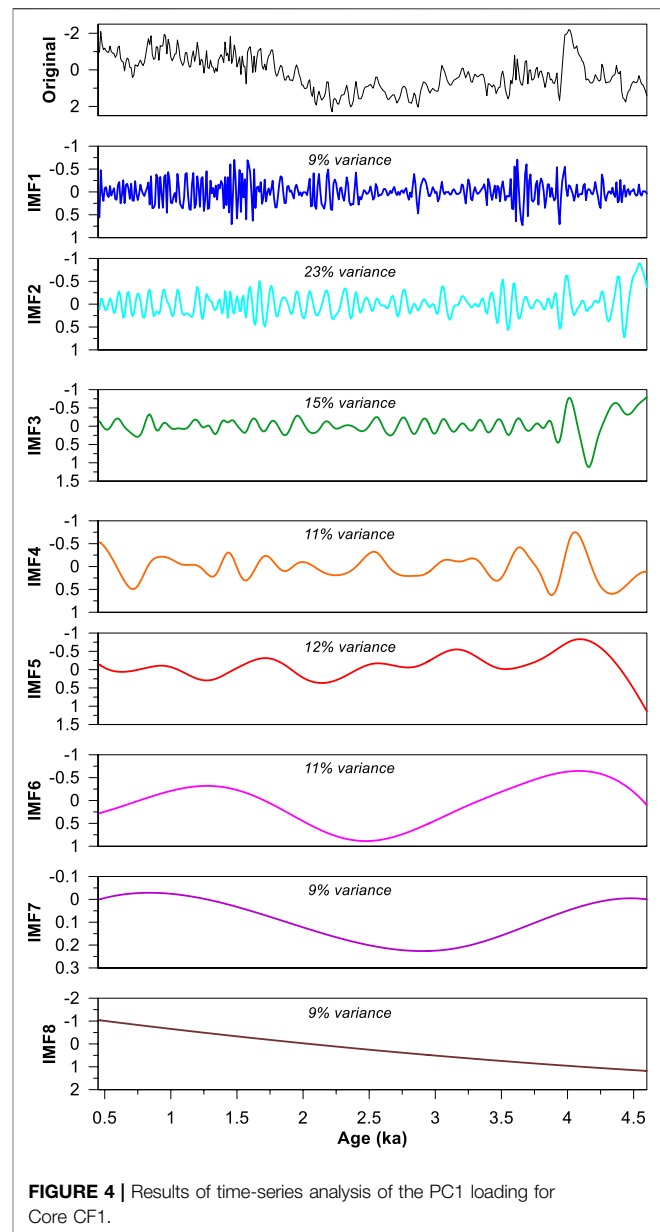
before 1950 CE (cal BP) using the Marine20 calibration curve (Heaton et al., 2020) and the ΔR value of 29 ± 18 a (Table 1). Default values for bootstrapping percentage and sedimentation rate uncertainty were set to 20% and 0.1 cm yr^{-1} , respectively. The sedimentation rate of Core CF1 varied from 45 cm/kyr to 190 cm/kyr, with an average value of ~ 90 cm/kyr.

2.2 Grain Size Analysis

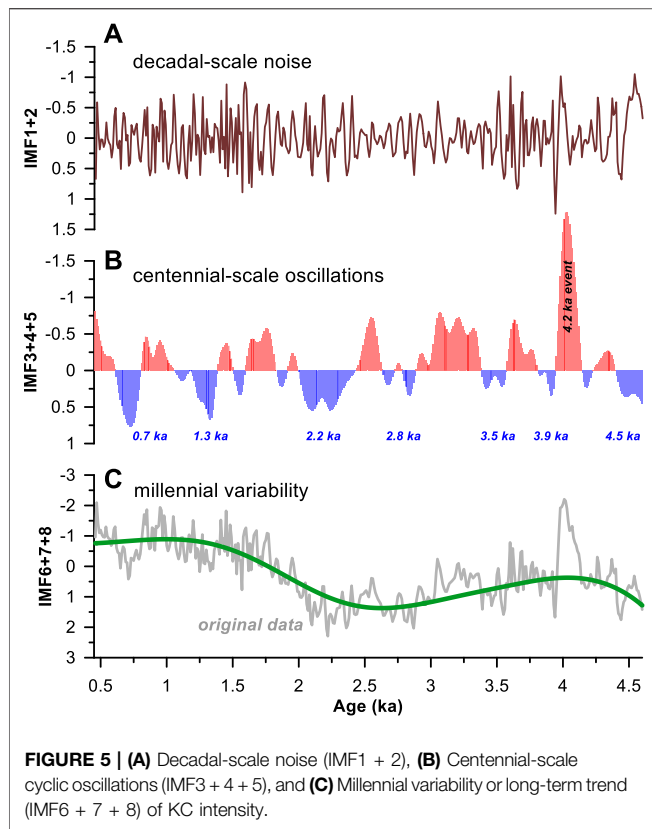
Grain-size analysis was conducted using a Mastersizer-2000 laser particle-size analyzer at Qingdao Institute of Marine Geology, China Geological Survey, with a measurement range of 0.02–2,000 μm and a size resolution of 0.01ϕ . The measuring error was within 3%. Before the grain-size analyses, the samples were pretreated with 10% H_2O_2 and 0.5 mol/L HCl for 24 h to remove organic matter and biogenic carbonate, respectively. The high-resolution analysis provided a resolution of ~ 12 years on average, with a lower resolution of ~ 22 years for the interval between 2,400 and 3,460 years BP.

Varimax-Rotated Principal Component Analysis

Varimax-rotated Principal Component Analysis (V-PCA) is a statistical procedure that uses orthogonal transformation to



convert a set of possibly correlated variables into a set of linearly uncorrelated variables called principal components. This method allowed us to separate out orthogonal modes and independent grain-size spectra from the grain size matrix that are related to potential input functions and sensitive to specific transport mechanisms (Darby et al., 2009; Hu et al., 2012; Yi et al., 2012; Zheng et al., 2014; Zheng et al., 2016). It has been used to successfully identify the transport mechanisms of the Yellow Sea (Hu et al., 2012) and the Okinawa Trough (Zheng et al., 2014; Zheng et al., 2016). In this study, V-PCA was applied to temporal variation of Core CF1 grain size spectrum with the input grain size matrix ranging from 0.41 to 707 μm . The mode of each extracted grain size component is defined as the grain size sets with largest factor loading, which is most representative for the grain size spectra (Figure 3).



Ensemble Empirical Mode Decomposition

The ensemble empirical mode decomposition (EEMD) method is based on the noise-assisted data analysis, which takes the average value of multiple measurements and obtains the ensemble means of corresponding intrinsic model functions (IMFs) as the results (Wu and Huang, 2009). EEMD is implemented through a sifting process that uses only local extrema. A complete sifting process stops when the residue becomes a monotonic function from which no more IMFs can be extracted. The total number of IMFs of a data set is close to $\log_2 N$ (N is the number of total data points). Detail process and explanation can be found in the MATLAB EEMD code program instructions (Wu and Huang, 2009). Before performing the EEMD, the PC1 loading of Core CF1 is linearly interpolated at a 10-years interval. Eight IMFs are generated from our data by the EEMD method and spectral analyses is applied to determine the periodicities and periodic stabilities using the PAST software (details can be found in <https://palaeo-electronica.org>) (Figure 4). We aim to quantify the relative contributions of both the long-term trend and centennial-scale oscillations. Considering the sample resolution used in this study, the IMF1 and IMF2 components with periodicity less than 100 years are thus considered as decadal-scale noise (Figure 5A). At the same time, the IMF3, IMF4, and IMF5 components exhibit centennial-scale cyclic oscillations with a total variance of 39% (Figure 5B), while the IMF6, IMF7, and IMF8 components are regarded as millennial variability or long-term trend, contributing altogether 29% to the total variance (Figure 5C).

RESULTS AND DISCUSSION

Paleoenvironment Implications of End-Members

Previous studies suggested the Okinawa Trough has multiple potential terrigenous sediment sources, mainly including the large rivers in China (Yellow and Yangtze Rivers) and small mountain rivers in Taiwan and Kyushu Islands, all of which display large temporal-spatial variations influenced by sea-level fluctuations, oceanic circulations, and East Asian monsoons over the last glacial-interglacial cycles (Dou et al., 2010; Dou et al., 2012; Wang et al., 2015; Dou et al., 2016; Beny et al., 2018; Li et al., 2019; Xu et al., 2019; Hu et al., 2020). Based on the results of previous studies, the sediment source-to-sink process in the ECS-Okinawa Trough since the LGM can be broadly summarized as follows: During the glacial periods marked by the low sea level (e.g., about 135 m below the present sea level during the LGM), the paleo-channels of Yellow and Yangtze Rivers were located on the YS and ECS shelves and may have directly entered the northern and middle regions of the Okinawa Trough, respectively. In contrast, Taiwan-derived sediments are confined to the southern region of the Okinawa Trough due to the weak or even absent KC during the glacial periods. Subsequently, sea level gradually rose from -135 m to -40 m during the deglaciation period (22–10 ka), resulting in the YS and ECS shelves being flooded by seawater along with the paleo-mouths of Yellow and Yangtze River which retreated quickly towards the YS shelf. During the process of sea level rise, terrigenous sediment supply became trapped on the shelf, although more intense continental erosion occurred resulting from the strengthened East Asian Summer Monsoon (EASM). Meanwhile, deglaciation transgression caused some reworked materials to be released from the ECS shelf into the Okinawa Trough, forming a broad tidal sand ridge covering the ECS middle-outer shelf. Conversely, the mainstream of the KC gradually deflected to the west of the Ryukyu Islands due to the rapid sea-level rise and then delivered the Taiwan Rivers sediment northward during this period. Provenance proxies indicated a significant change from a dominance of the paleo-Yangtze or paleo-Yellow River to an increased influence from Taiwanese rivers after 9–10 ka or ~7 ka, associated with the establishment of a “water barrier” of strong KC intensity and a modern circulation pattern since then. Combining the results of previous studies, it can be found that the sea level has stabilized or changed very little and the ocean circulation system of ECS has been formed since the Late Holocene. At that time, the sediment transport dynamics affecting the middle Okinawa Trough are mainly controlled by changes in the strength of the KC.

For Core CF1, results of the V-PCA analyses on the grain-size matrix are shown in Figure 2A. Three principal grain-size components (PC1: 69%, PC2: 16%, and PC3: 10%) were identified for Core CF1, which totally account for 95% of the variance. The first mode (PC1) has a broad negative peak at 4–16 μm and a positive peak at 32–148 μm (Figure 2A). The second mode (PC2) has a positive peak at 0.4–3.2 μm and a trough around 18–26 μm (Figure 2A). The third mode (PC3) has a strongly positive peak at 297–707 μm

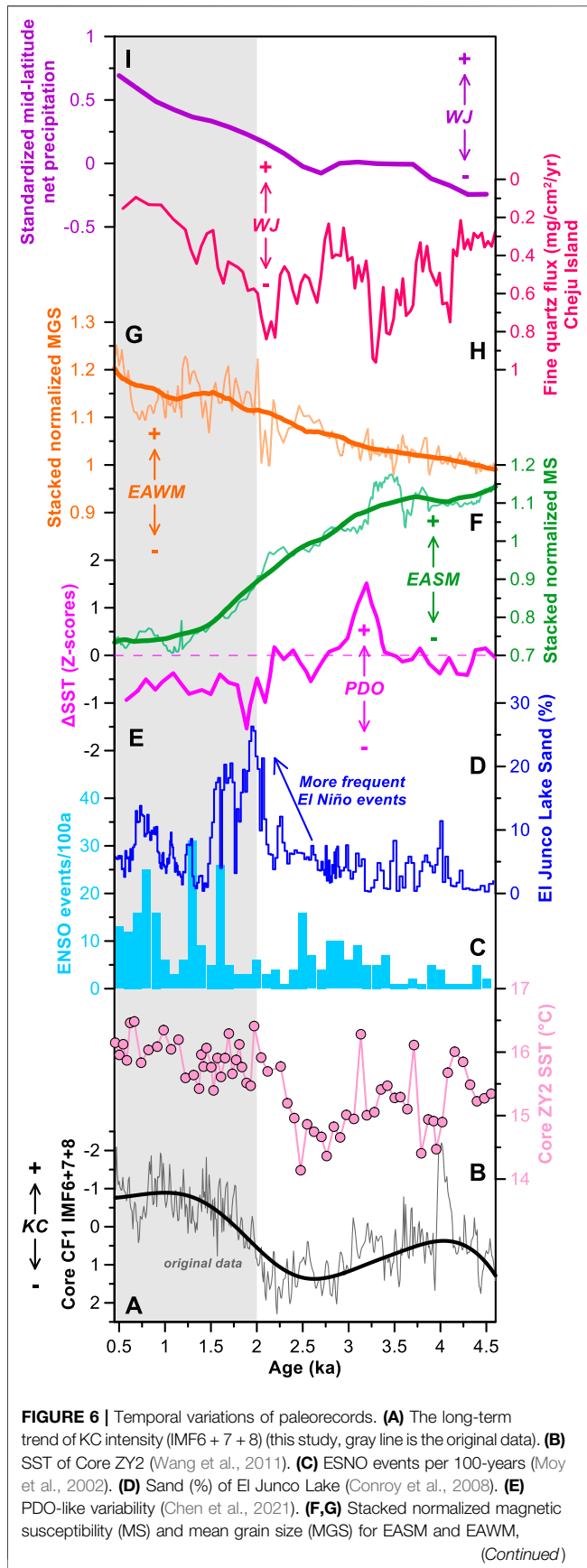


FIGURE 6 | Temporal variations of paleorecords. **(A)** The long-term trend of KC intensity (IMF6 + 7 + 8) (this study, gray line is the original data). **(B)** SST of Core ZY2 (Wang et al., 2011). **(C)** ENSO events per 100-years (Moy et al., 2002). **(D)** Sand (%) of El Junco Lake (Conroy et al., 2008). **(E)** PDO-like variability (Chen et al., 2021). **(F,G)** Stacked normalized magnetic susceptibility (MS) and mean grain size (MGS) for EASM and EAWM, respectively, (Kang et al., 2020). **(H)** Fine quartz flux deposited at Cheju Island (Lim and Matsumoto, 2006, 2008). **(I)** Standardized, average mid-latitude (30°N–50°N) net precipitation (Routson et al., 2019).

(Figure 2A). Two nearby cores A7 and OKI02 gave the same modes with a consistent grain size structure, and such consistency strongly indicates that there must be identifiable mechanisms to account for these specific modes (Zheng et al., 2014; Zheng et al., 2016). As suggested by Zheng et al. (2014, 2016), three PCs of the Okinawa Trough cores (A7 and OKI02) were interpreted as KC silt (PC1), bottom nepheloid clay (PC2), and turbidity sand (PC3), respectively. Sr-Nd isotopic compositions of 5–18 μm fractions from Core AF2/OF3 were further compared with the potential endmembers (the Yangtze River, Yellow River, and rivers of Taiwan Island) to assess the provenance, which clearly indicated that the 5–18 μm fractions originated from rivers of Taiwan Island and are transported by, and sensitive to, the strength of the KC (Zheng et al., 2016). Specially, sea level has stabilized or changed very little and the ocean circulation system of ECS has been formed since the Middle Holocene, and at that time, the sediment transport dynamics affecting the middle Okinawa Trough are mainly controlled by changes in the strength of the KC (Zheng et al., 2014; Zheng et al., 2016). These lines of evidence support the interpretation of PC1 loading of Core CF1 as a dynamic proxy for the KC intensity.

Long-Term Trend of Kuroshio Current During the Late Holocene and Potential Influences Mechanisms

To quantify the relative contributions of long-term trend and centennial-scale oscillations of the KC, we performed a noise-assisted data analysis EEMD on the PC1 loading of Core CF1 after linearly interpolated at a 10-years interval. Based on the results of the EEMD, we combined the IMF6, IMF7 and IMF8 components (IMF6+7 + 8) to reveal the millennial variability or long-term trend of KC intensity (Figure 6A). Our reconstruction of the KC intensity contradicts recent inferences based on low-resolution magnetic parameters and paired organic paleothermometers (Li et al., 2019; Li et al., 2020), but is consistent with several other lines of evidence. For example, abundance of *P. obliquiloculata* (Jian et al., 2000; Lin et al., 2006; Xiang et al., 2007), sediment mercury (Hg) enrichment factor (Lim et al., 2017), and sediment provenance changes (Jiang et al., 2019; Xu et al., 2019), as well as SST variations in the South Yellow Sea (Wang et al., 2011; Jia et al., 2019) (Figure 6B). Within the age uncertainty estimates, our IMF6+7 + 8 record of Core CF1 is broadly consistent with the abovementioned proxy evidence and suggests a slow-down of the KC during the period of 4.6–2.0 ka, followed by quickly enhanced KC and attaining the highest level at approximately 0.5 ka (Figure 6A). Additionally, climate records from the Taiwan Island (Selvaraj et al., 2007; Wang et al., 2015; Ding et al., 2020),

Cheju Island (Park et al., 2016; Park, 2017) and Northeastern Asia (Hong et al., 2005; Zhao et al., 2021) reflect gradual precession-driven cooling/drying since the Early-Middle Holocene with rapid climate amelioration since ~ 2.0 ka. Their similarity to the KC intensity evolution suggests the KC transports huge amounts of latent heat and water vapor to the atmosphere along its path and plays an important role in modulating surrounding climate change.

What, then, explains Late Holocene KC evolution? Firstly, although a few uncertainties remain with respect to the Holocene ENSO activities, most of the records support a strong relationship between ENSO variability and the Equatorial Pacific mean state and suggests more frequent El Niño events during the Late Holocene (Figures 6C,D) (Moy et al., 2002; Conroy et al., 2008; Koutavas and Joanides, 2012; Sadekov et al., 2013; Gill et al., 2016; Barr et al., 2019). Enhanced El Niño activities during the Late Holocene, characterized by weakened Walker circulation and northernmost position of NEC bifurcation latitude, is not conducive to KC reinforcement at that time.

Secondly, the variability of the KC along the ECS margin at interdecadal scales is more closely related to PDO than to ENSO, and KC generally decelerated during the negative PDO phase, and vice versa (Andres et al., 2009; Wu, 2013; Wu et al., 2019). Recent study shows that PDO-like pattern shifts from a positive to a negative phase at ~ 2 ka based on $\Delta\text{SST}_{\text{E-W}}$ between Cores MD01-2,412 and ODP1019C (Figure 6E) (Chen et al., 2021). Similar results are also found in the PDO record from the Santa Barbara Basin over the last 2,700 years (Beaufort and Grelaud, 2017). Commonly, negative PDO phase since ~ 2 ka, characterized by decreased negative wind stress curl (WSC), should decelerate the southward Sverdrup flow in the subtropical gyre and thus weaken return flow (i.e., KC), which conflicts with the KC records from the Okinawa Trough.

Finally, the East Asian monsoon systems, including the southeasterly EASM and the northwesterly East Asian Winter Monsoon (EAWM), are another important factor influencing the variation of KC intensity (Jian et al., 2000; Zheng et al., 2016). High-resolution reconstruction of EASM and EAWM from three loess sections in the Loess Plateau display continuously weakened EASM (Figure 6F) and persistently strengthened EAWM during the Late Holocene (Figure 6G) (Kang et al., 2020). These situations would trigger less negative or even positive WSC over the North Pacific subtropics, suppressing the KC intensity, which also contradicts the enhanced KC since ~ 2.0 ka.

Overall, low-latitude processes (e.g., East Asian monsoons and/or changes in ENSO/PDO-like phases) should be a secondary factor or negligible for the long-term trend of the KC intensity on millennial timescale during the Late Holocene.

Westerly Driven North Pacific Subtropical Gyre Variations During the Late Holocene

As discussed earlier, forcings other than low-latitude processes are required to explain the long-term trend of the KC intensity

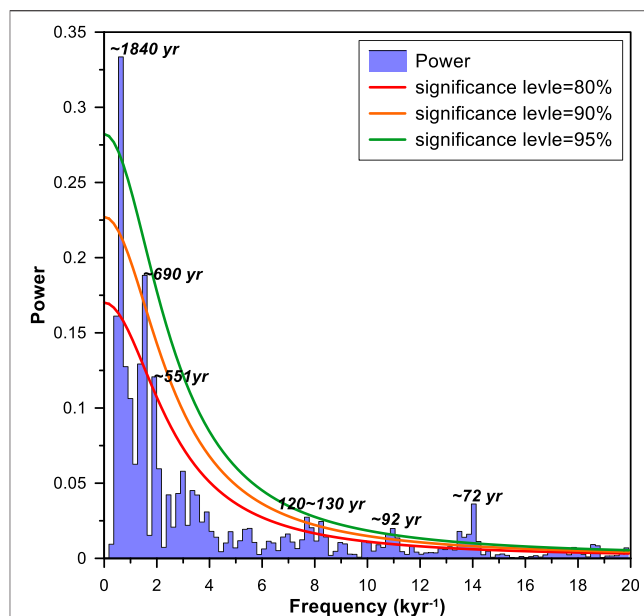
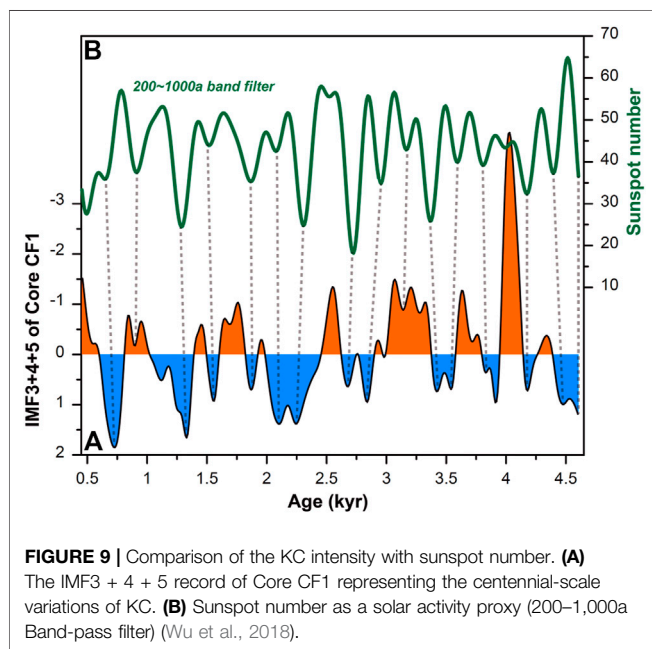
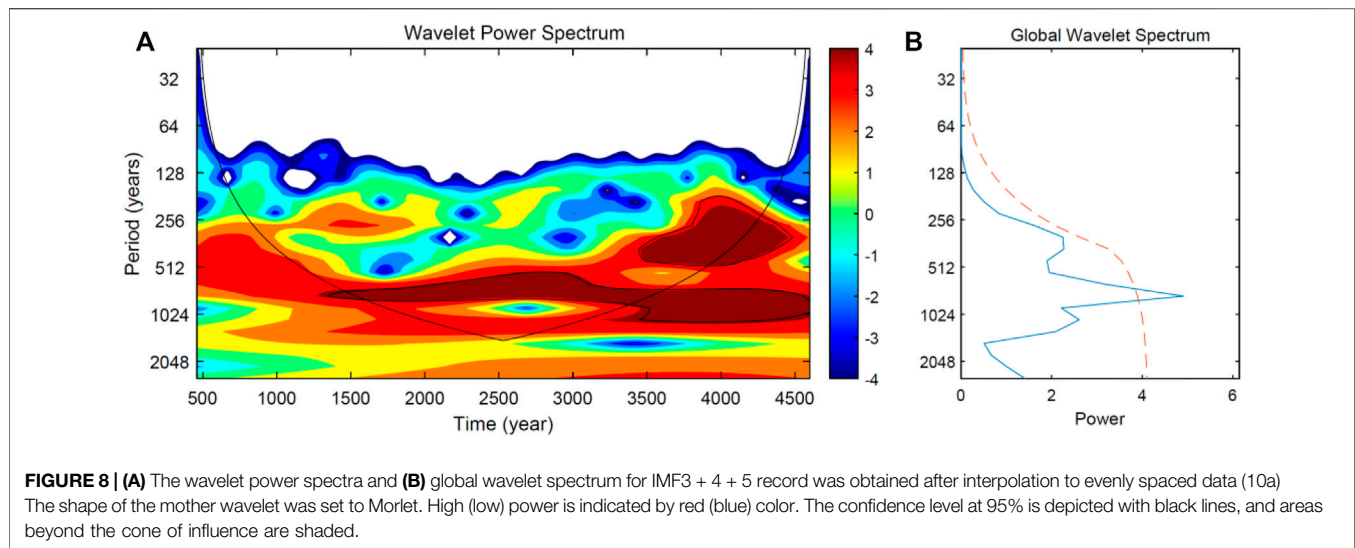


FIGURE 7 | Results of cyclicity analysis of the original PC1 record.

during the Late Holocene. Indeed, the KC is driven by a basin-scale negative WSC over the North Pacific, depending on the combined effects of subtropical easterly and mid-latitude westerly winds (Seager and Simpson, 2016). Enhanced negative WSC over the North Pacific forces stronger southward Sverdrup flow in the inner ocean, which is compensated by strengthened northward flow of the KC at the western boundary (Seager and Simpson, 2016). Accordingly, we hypothesize that the mid-latitude Westerly Jet (WJ) and its associated WSC in the North Pacific play a dominant role in the long-term trend of KC intensity since the Late Holocene. Recent studies have highlighted teleconnections between North Pacific atmospheric and oceanic circulations over the glacial-interglacial cycles, with equatorward (poleward) and intensified (weaker) WJ during the glacial (interglacial) periods, coupling with the expansion and strengthening of circulation gyres during cold periods and vice versa (Gray et al., 2018; Gray et al., 2020; Abell et al., 2021).

Moreover, dust records from the Tarim Basin (Han et al., 2019), the Cheju Island (Lim and Matsumoto, 2006, 2008), and the Japan Sea (Nagashima et al., 2013) suggested strengthening and southward shift of WJ occurred during the Late Holocene (Figure 6H), which is further confirmed by Holocene spatiotemporal precipitation patterns (Figure 6I) and climate model simulations (Chen et al., 2019; Herzsuh et al., 2019; Routson et al., 2019; Zhou et al., 2020). The forcing mechanism may be that seasonal difference between the winter and summer insolation across the latitudes results in gradually increased pole-to-equator thermal gradient during the Late Holocene (Chen et al., 2019; Routson et al., 2019). Thus, we provide direct evidence for the predominance of accelerating and southward shift of mid-latitude WJ, rather than low-latitude processes, causing more negative WSC over the North Pacific and thus stronger KC since ~ 2 ka.



Solar Forcing of Centennial-Scale Variability of Kuroshio Current

Superimposed on the long-term trend of the KC is significant centennial-scale variability, which displays a larger amplitude and a longer anomaly duration after ~ 2.5 ka (Figure 5B). We found a periodicity of $\sim 1,800$ -years (at the 95% significance level), ~ 700 -years (at the 90% significance level) and ~ 500 -years (at the 95% significance level) of the original PC1 record from Core CF1 by the PAST software (Figure 7). However, it seems inappropriate to determine the 1,800-years cycle as one of the credible climate oscillations due to their insufficient temporal length of the original PC1 records. We therefore consider only the 500–700-year cycles because of underlying solar forcing. Moreover, we also performed wavelet power spectrum analyses on the IMF3+4 + 5

record and reflected statistically significant centennial periodicities on approximately 500-years and 700-years ($>90\%$ confidence level) (Figure 8). Similar periodicities are also found in the solar activity records and exhibit strong power after ~ 2.5 ka (Wanner et al., 2008; Steinhilber et al., 2012). This further suggests a link between the KC variability and solar activity on a centennial-scale, with reduced solar activity corresponding with weak KC intensity (Figure 9). Not all KC weakening events covary with sunspot number (SN) on a centennial-scale for the Late Holocene, which may stem from age model uncertainties and sampling resolution.

Previous studies highlight that solar variability (500–700-year cycles), amplified by low-latitude oceanic-atmospheric interactions (e.g., ENSO), could have played an important role in regulating centennial-scales climate variations (Liu et al., 2014; Zhu et al., 2017; Xu et al., 2019; Xu et al., 2020). Model simulations suggest that the ENSO system acts as a mediator of solar activities on the climate system's low-latitude heat engine (Emile-Geay et al., 2007). This has been further confirmed by paleoclimate reconstructions, which show that the tropical Pacific mean states shift in response to the solar activities of the last 1,500 years (Mann et al., 2009), for the early-middle Holocene (Marchitto et al., 2010), as well as the entire Holocene (Ersek et al., 2012). In addition, solar irradiance variations can also trigger changes in the strength and direction of WJ across the North Atlantic via a “top-down” mechanism (Ineson et al., 2011), with the southward migration and enhanced intensity of WJ responding to lower solar irradiance (Olsen et al., 2012; Wirth et al., 2013; Lan et al., 2020). Nonetheless, if some direct (though amplified) solar forcing of the WJ was the dominant control on the KC intensity, we would expect enhancement of KC intensity correlated with reduced solar activity, conflicting with the fact observed (Figure 3). Taken together, we can conclude that, since the Late Holocene, weak solar irradiation makes the tropical Pacific to be an El Niño-like state, associated with weakened easterly trade winds and attenuated EASM, which

overwhelms the enhanced intensity of mid-latitude WJ and contributes to the decreased KC intensity on centennial-scale.

SUMMARY

New 1-cm contiguous grain size data from Core CF1 provide new insights into Late Holocene millennial-to centennial-scale KC variability. We interpret the long-term trend of the KC as a response to the strengthening and southward shift of WJ during the Late Holocene, resulting from gradual enhanced pole-to-equator thermal gradient forced by orbital forcing mechanisms. However, the waxing and waning of solar activities, via changes in Walker circulation and ENSO of the tropical Pacific, have an overwhelming influence on the centennial-scale changes of the KC intensity. Our findings thus, highlight those two regions, the high-mid latitude and tropical Pacific, alternate their dominance as source regions causing the dynamic changes of the KC at different timescales.

Recent evidence suggests that the WBCs have strengthened and shifted toward the poles due to global warming during the past few decades, which is consistent with the centennial-scale changes of KC intensity forced by solar activity. However, if global warming continues, especially with the Arctic amplification, we hypothesize that the WBCs may be in turn decrease once the threshold is breached, as shown by the long-term trend of KC during the Late Holocene. Further comprehensive climate model research is necessary to understand how the KC responds to different forcing

mechanisms under a continuous global warming scenario, which is crucial to the reliable prediction of the future climate changes in East Asia.

DATA AVAILABILITY STATEMENT

The raw data supporting the conclusion of this article will be made available by the authors, without undue reservation.

AUTHOR CONTRIBUTIONS

BH and JL designed the project and developed the conceptual framework. XD collected the AMS 14C dating materials and wrote the manuscript. JZ and QL analyzed sediment grain size. YY performed the EEMD analysis. JL, XZ, and LY were involved in the interpretation of the results.

FUNDING

This research was jointly supported by the National Natural Science Foundation of China (No. 41976192), the Strategic Priority Research Program of Chinese Academy of Sciences (No. XDB40000000), the National Key Research and Development Program of China (No. 2018YFC0310001), Shandong Province Natural Science Foundation (No. ZR202103010094), the Project of China Geological Survey (No. DD20191010).

REFERENCES

- Abell, J. T., Winckler, G., Anderson, R. F., and Herbert, T. D. (2021). Poleward and Weakened Westerlies during Pliocene Warmth. *Nature* 589 (7840), 70–75. doi:10.1038/s41586-020-03062-1
- Andres, M., Park, J.-H., Wimbush, M., Zhu, X.-H., Nakamura, H., Kim, K., et al. (2009). Manifestation of the Pacific Decadal Oscillation in the Kuroshio. *Geophys. Res. Lett.* 36, L16602. doi:10.1029/2009gl039216
- Barr, C., Tibby, J., Leng, M. J., Tyler, J. J., Henderson, A. C. G., Overpeck, J. T., et al. (2019). Holocene El Niño-Southern Oscillation Variability Reflected in Subtropical Australian Precipitation. *Scientific Rep.* 9 (1), 1627. doi:10.1038/s41598-019-38626-3
- Beaufort, L., and Grelaud, M. (2017). A 2700-year Record of ENSO and PDO Variability from the Californian Margin Based on Coccolithophore Assemblages and Calcification. *Prog. Earth Planet. Sci.* 4 (1), 5. doi:10.1186/s40645-017-0123-z
- Beny, F., Toucanne, S., Skonieczny, C., Bayon, G., and Ziegler, M. (2018). Geochemical Provenance of Sediments from the Northern East China Sea Document a Gradual Migration of the Asian Monsoon belt over the Past 400,000 Years. *Quat. Sci. Rev.* 190, 161–175. doi:10.1016/j.quascirev.2018.04.032
- Chen, F., Chen, J., Huang, W., Chen, S., Huang, X., Jin, L., et al. (2019). Westerlies Asia and Monsoonal Asia: Spatiotemporal Differences in Climate Change and Possible Mechanisms on Decadal to Sub-orbital Timescales. *Earth-Sci. Rev.* 192, 337–354. doi:10.1016/j.earscirev.2019.03.005
- Chen, C., Zhao, W., and Zhang, X. (2021). Pacific Decadal Oscillation-like Variability at a Millennial Timescale during the Holocene. *Glob. Planet. Change* 199, 103448. doi:10.1016/j.gloplacha.2021.103448
- Conroy, J. L., Overpeck, J. T., Cole, J. E., Shanahan, T. M., and Steinitz-Kannan, M. (2008). Holocene Changes in Eastern Tropical Pacific Climate Inferred from a Galápagos lake Sediment Record. *Quat. Sci. Rev.* 27 (11–12), 1166–1180. doi:10.1016/j.quascirev.2008.02.015
- Darby, D. A., Ortiz, J., Polyak, L., Lund, S., Jakobsson, M., and Woodgate, R. A. (2009). The Role of Currents and Sea Ice in Both Slowly Deposited central Arctic and Rapidly Deposited Chukchi–Alaskan Margin Sediments. *Glob. Planet. Change* 68 (1–2), 58–72. doi:10.1016/j.gloplacha.2009.02.007
- Xu, D., Lu, H., Chu, G., Liu, L., Shen, C., Li, F., et al. (2019). Synchronous 500-year Oscillations of Monsoon Climate and Human Activity in Northeast Asia. *Nat. Commun.* 10, 4105. doi:10.1038/s41467-019-12138-0
- Ding, X., Zheng, L., Zheng, X., and Kao, S.-J. (2020). Holocene East Asian Summer Monsoon Rainfall Variability in Taiwan. *Front. Earth Sci.* 8, 234. doi:10.3389/feart.2020.00234
- Dou, Y., Yang, S., Liu, Z., Clift, P. D., Shi, X., Yu, H., et al. (2010). Provenance Discrimination of Siliciclastic Sediments in the Middle Okinawa Trough since 30ka: Constraints from Rare Earth Element Compositions. *Mar. Geol.* 275 (1–4), 212–220. doi:10.1016/j.margeo.2010.06.002
- Dou, Y., Yang, S., Liu, Z., Shi, X., Li, J., Yu, H., et al. (2012). Sr–Nd Isotopic Constraints on Terrigenous Sediment Provenances and Kuroshio Current Variability in the Okinawa Trough during the Late Quaternary. *Palaeogeography, Palaeoclimatology, Palaeoecology* 365–366, 38–47. doi:10.1016/j.palaeo.2012.09.003
- Dou, Y., Yang, S., Shi, X., Clift, P. D., Liu, S., Liu, J., et al. (2016). Provenance Weathering and Erosion Records in Southern Okinawa Trough Sediments since 28ka: Geochemical and Sr–Nd–Pb Isotopic Evidences. *Chem. Geology* 425, 93–109. doi:10.1016/j.chemgeo.2016.01.029
- Emile-Geay, J., Cane, M., Seager, R., Kaplan, A., and Almasi, P. (2007). El Niño as a Mediator of the Solar Influence on Climate. *Paleoceanography* 22, PA3210. doi:10.1029/2006PA001304
- England, M. H., McGregor, S., Spence, P., Meehl, G. A., Timmermann, A., Cai, W., et al. (2014). Recent Intensification of Wind-Driven Circulation in the Pacific and the Ongoing Warming Hiatus. *Nat. Clim. Change* 4 (3), 222–227. doi:10.1038/nclimate2106

- Ersek, V., Clark, P. U., Mix, A. C., Cheng, H., and Lawrence Edwards, R. (2012). Holocene winter Climate Variability in Mid-Latitude Western North America. *Nat. Commun.* 3 (1), 1219. doi:10.1038/ncomms2222
- Gill, E. C., Rajagopalan, B., Molnar, P., and Marchitto, T. M. (2016). Reduced-dimension Reconstruction of the Equatorial Pacific SST and Zonal Wind fields over the Past 10,000 Years Using Mg/Ca and Alkenone Records. *Paleoceanography* 31 (7), 928–952. doi:10.1002/2016PA002948
- Gray, W. R., Rae, J. W. B., Wills, R. C. J., Shevenell, A. E., Taylor, B., Burke, A., et al. (2018). Deglacial Upwelling, Productivity and CO₂ Outgassing in the North Pacific Ocean. *Nat. Geosci.* 11 (5), 340–344. doi:10.1038/s41561-018-0108-6
- Gray, W. R., Wills, R. C. J., Rae, J. W. B., Burke, A., Ivanovic, R. F., Roberts, W. H. G., et al. (2020). Wind-Driven Evolution of the North Pacific Subpolar Gyre over the Last Deglaciation. *Geophys. Res. Lett.* 47, e2019GL086328. doi:10.1029/2019gl086328
- Han, W., Lü, S., Appel, E., Berger, A., Madsen, D., Vandenberghe, J., et al. (2019). Dust Storm Outbreak in Central Asia after ~3.5 Kyr BP. *Geophys. Res. Lett.* 46 (13), 7624–7633. doi:10.1029/2018GL081795
- Heaton, T. J., Köhler, P., Butzin, M., Bard, E., Reimer, R. W., Austin, W. E. N., et al. (2020). Marine20—The Marine Radiocarbon Age Calibration Curve (0–55,000 Cal BP). *Radiocarbon* 62 (4), 779–820. doi:10.1017/rdc.2020.68
- Herzschuh, U., Cao, X., Laepple, T., Dallmeyer, A., Telford, R. J., Ni, J., et al. (2019). Position and Orientation of the westerly Jet Determined Holocene Rainfall Patterns in China. *Nat. Commun.* 10 (1), 2376. doi:10.1038/s41467-019-09866-8
- Hong, Y. T., Hong, B., Lin, Q. H., Shibata, Y., Hirota, M., Zhu, Y. X., et al. (2005). Inverse Phase Oscillations between the East Asian and Indian Ocean Summer Monsoons during the Last 2000 Years and Paleo-El Niño. *Earth Planet. Sci. Lett.* 231 (3), 337–346. doi:10.1016/j.epsl.2004.12.025
- Hu, B., Yang, Z., Zhao, M., Saito, Y., Fan, D., and Wang, L. (2012). Grain Size Records Reveal Variability of the East Asian Winter Monsoon since the Middle Holocene in the Central Yellow Sea Mud Area, China. *Sci. China Earth Sci.* 55 (10), 1656–1668. doi:10.1007/s11430-012-4447-7
- Hu, D., Wu, L., Cai, W., Gupta, A. S., Ganachaud, A., Qiu, B., et al. (2015). Pacific Western Boundary Currents and Their Roles in Climate. *Nature* 522 (7556), 299–308. doi:10.1038/nature14504
- Hu, S., Zeng, Z., Fang, X., Yin, X., Chen, Z., Li, X., et al. (2020). Increasing Terrigenous Sediment Supply from Taiwan to the Southern Okinawa Trough over the Last 3000 Years Evidenced by Sr Nd Isotopes and Geochemistry. *Sediment. Geol.* 406, 105725. doi:10.1016/j.sedgeo.2020.105725
- Ineson, S., Scaife, A. A., Knight, J. R., Manners, J. C., Dunstone, N. J., Gray, L. J., et al. (2011). Solar Forcing of winter Climate Variability in the Northern Hemisphere. *Nat. Geosci.* 4 (11), 753–757. doi:10.1038/ngeo1282
- Jia, Y., Li, D.-W., Yu, M., Zhao, X., Xiang, R., Li, G., et al. (2019). High- and Low-Latitude Forcing on the South Yellow Sea Surface Water Temperature Variations during the Holocene. *Glob. Planet. Change* 182, 103025. doi:10.1016/j.gloplacha.2019.103025
- Jian, Z., Wang, P., Saito, Y., Wang, J., PÉaumann, U., Ob, T., et al. (2000). Holocene Variability of the Kuroshio Current in the Okinawa Trough, Northwestern Pacific Ocean. *Earth Planet. Sci. Lett.* 184, 305–319. doi:10.1016/s0012-821x(00)00321-6
- Jiang, F., Xiong, Z., Frank, M., Yin, X., and Li, A. (2019). The Evolution and Control of Detrital Sediment Provenance in the Middle and Northern Okinawa Trough since the Last Deglaciation: Evidence from Sr and Nd Isotopes. *Palaeogeography, Palaeoclimatology, Palaeoecology* 522, 1–11. doi:10.1016/j.palaeo.2019.02.017
- Wang, J., Li, A., Xu, K., Zheng, X., and Huang, J. (2015). Clay mineral and Grain Size Studies of Sediment Provenances and Palaeoenvironment Evolution in the Middle Okinawa Trough since 17ka. *Mar. Geol.* 366, 49–61. doi:10.1016/j.margeo.2015.04.007
- Kang, S., Du, J., Wang, N., Dong, J., Wang, D., Wang, X., et al. (2020). Early Holocene Weakening and Mid- to Late Holocene Strengthening of the East Asian winter Monsoon. *Geology* 48 (11), 1043–1047. doi:10.1130/g47621.1
- Koutavas, A., and Joanides, S. (2012). El Niño-Southern Oscillation Extrema in the Holocene and Last Glacial Maximum. *Paleoceanography* 27, PA4208. doi:10.1029/2012pa002378
- Lan, J., Zhang, J., Cheng, P., Ma, X., Ai, L., Chawchai, S., et al. (2020). Late Holocene Hydroclimatic Variation in central Asia and its Response to Mid-latitude Westerlies and Solar Irradiance. *Quat. Sci. Rev.* 238, 106330. doi:10.1016/j.quascirev.2020.106330
- Li, Q., Zhang, Q., Li, G., Liu, Q., Chen, M.-T., Xu, J., et al. (2019). A New Perspective for the Sediment Provenance Evolution of the Middle Okinawa Trough since the Last Deglaciation Based on Integrated Methods. *Earth Planet. Sci. Lett.* 528, 115839. doi:10.1016/j.epsl.2019.115839
- Li, Q., Li, G., Chen, M. T., Xu, J., Liu, S., and Chen, M. (2020). New Insights into Kuroshio Current Evolution since the Last Deglaciation Based on Paired Organic Paleothermometers from the Middle Okinawa Trough. *Paleoceanogr. Paleoclimatol.* 35, e2020PA004140. doi:10.1029/2020pa004140
- Wang, L.-C., Behling, H., Kao, S.-J., Li, H.-C., Selvaraj, K., Hsieh, M.-L., et al. (2015). Late Holocene Environment of Subalpine Northeastern Taiwan from Pollen and Diatom Analysis of lake Sediments. *J. Asian Earth Sci.* 114, 447–456. doi:10.1016/j.jseas.2015.03.037
- Lim, J., and Matsumoto, E. (2006). Bimodal Grain-Size Distribution of Aeolian Quartz in a Maar of Cheju Island, Korea, during the Last 6500 years: Its Flux Variation and Controlling Factor. *Geophys. Res. Lett.* 33 (21). doi:10.1029/2006GL027432
- Lim, J., and Matsumoto, E. (2008). Fine Aeolian Quartz Records in Cheju Island, Korea, during the Last 6500 Years and Pathway Change of the Westerlies over East Asia. *J. Geophys. Res. Atmos.* 113, D08106. doi:10.1029/2007JD008501
- Lim, D., Kim, J., Xu, Z., Jeong, K., and Jung, H. (2017). New Evidence for Kuroshio Inflow and deepwater Circulation in the Okinawa Trough, East China Sea: Sedimentary Mercury Variations over the Last 20 Kyr. *Paleoceanography* 32 (6), 571–579. doi:10.1002/2017pa003116
- Lin, Y.-S., Wei, K.-Y., Lin, I.-T., Yu, P.-S., Chiang, H.-W., Chen, C.-Y., et al. (2006). The Holocene Pulleniatina Minimum Event Revisited: Geochemical and Faunal Evidence from the Okinawa Trough and Upper Reaches of the Kuroshio Current. *Mar. Micropaleontol.* 59 (3-4), 153–170. doi:10.1016/j.marmicro.2006.02.003
- Liu, Z., Lu, Z., Wen, X., Otto-Bliesner, B. L., Timmermann, A., and Cobb, K. M. (2014). Evolution and Forcing Mechanisms of El Niño over the Past 21,000 Years. *Nature* 515 (7528), 550–553. doi:10.1038/nature13963
- Lougheed, B. C., and Obrochta, S. P. (2019). A Rapid, Deterministic Age-Depth Modeling Routine for Geological Sequences with Inherent Depth Uncertainty. *Paleoceanogr. Paleoclimatol.* 34 (1), 122–133. doi:10.1029/2018PA003457
- Mann, M. E., Woodruff, J. D., Donnelly, J. P., and Zhang, Z. (2009). Atlantic Hurricanes and Climate Over the Past 1,500 Years. *Nature* 460 (7257), 880–883. doi:10.1038/nature08219
- Marchitto, T. M., Muscheler, R., Ortiz Joseph, D., Carriquiry Jose, D., and van Geen, A. (2010). Dynamical Response of the Tropical Pacific Ocean to Solar Forcing during the Early Holocene. *Science* 330 (6009), 1378–1381. doi:10.1126/science.1194887
- Moy, C. M., Seltzer, G. O., Rodbell, D. T., and Anderson, D. M. (2002). Variability of El Niño/Southern Oscillation Activity at Millennial Timescales during the Holocene Epoch. *Nature* 420 (6912), 162–165. doi:10.1038/nature01194
- Nagashima, K., Tada, R., and Toyoda, S. (2013). Westerly Jet-East Asian Summer Monsoon Connection during the Holocene. *Geochimistry, Geophysics. Geosystems* 14 (12), 5041–5053. doi:10.1002/2013gc004931
- Nakamura, H. (2020). “Changing Kuroshio and its Affected Shelf Sea: A Physical View,” in *Changing Asia-Pacific Marginal Seas*, 265–305. doi:10.1007/978-981-15-4886-4_15
- Olsen, J., Anderson, N. J., and Knudsen, M. F. (2012). Variability of the North Atlantic Oscillation over the Past 5,200 Years. *Nat. Geosci.* 5 (11), 808–812. doi:10.1038/ngeo1589
- Park, J., Shin, Y. H., and Byrne, R. (2016). Late-Holocene Vegetation and Climate Change in Jeju Island, Korea and its Implications for ENSO Influences. *Quat. Sci. Rev.* 153, 40–50. doi:10.1016/j.quascirev.2016.10.011
- Park, J. (2017). Solar and Tropical Ocean Forcing of Late-Holocene Climate Change in Coastal East Asia. *Palaeogeography, Palaeoclimatology, Palaeoecology* 469, 74–83. doi:10.1016/j.palaeo.2017.01.005
- Routson, C. C., McKay, N. P., Kaufman, D. S., Erb, M. P., Goosse, H., Shuman, B. N., et al. (2019). Mid-latitude Net Precipitation Decreased with Arctic Warming during the Holocene. *Nature* 568 (7750), 83–87. doi:10.1038/s41586-019-1060-3
- Sadekov, A. Y., Ganeshram, R., Pichevin, L., Berdin, R., McClymont, E., Elderfield, H., et al. (2013). Palaeoclimate Reconstructions Reveal a strong Link between El Niño-Southern Oscillation and Tropical Pacific Mean State. *Nat. Commun.* 4 (1), 2692. doi:10.1038/ncomms3692

- Seager, R., and Simpson, I. R. (2016). Western Boundary Currents and Climate Change. *J. Geophys. Res. Oceans* 121 (9), 7212–7214. doi:10.1002/2016JC012156
- Selvaraj, K., Chen, C. T. A., and Lou, J.-Y. (2007). Holocene East Asian Monsoon Variability: Links to Solar and Tropical Pacific Forcing. *Geophys. Res. Lett.* 34 (1). doi:10.1029/2006gl028155
- Steinhilber, F., Abreu, J. A., Beer, J., Brunner, I., Christl, M., Fischer, H., et al. (2012). 9,400 Years of Cosmic Radiation and Solar Activity from Ice Cores and Tree Rings. *Proc. Natl. Acad. Sci. U. S. A.* 109 (16), 5967–5971. doi:10.1073/pnas.1118965109
- Wang, L., Yang, Z., Zhang, R., Fan, D., Zhao, M., and Hu, B. (2011). Sea Surface Temperature Records of Core ZY2 from the central Mud Area in the South Yellow Sea during Last 6200 Years and Related Effect of the Yellow Sea Warm Current. *Chin. Sci. Bull.* 56 (15), 1588–1595. doi:10.1007/s11434-011-4442-y
- Wanner, H., Beer, J., Bütikofer, J., Crowley, T. J., Cubasch, U., Flückiger, J., et al. (2008). Mid- to Late Holocene Climate Change: an Overview. *Quat. Sci. Rev.* 27 (19), 1791–1828. doi:10.1016/j.quascirev.2008.06.013
- Wirth, S. B., Glur, L., Gilli, A., and Anselmetti, F. S. (2013). Holocene Flood Frequency across the Central Alps – Solar Forcing and Evidence for Variations in North Atlantic Atmospheric Circulation. *Quat. Sci. Rev.* 80, 112–128. doi:10.1016/j.quascirev.2013.09.002
- Wu, C. J., Usoskin, I. G., Krivova, N., Kovaltsov, G. A., Baroni, M., and Bard, E. (2018). Solar Activity Over Nine Millennia: A Consistent Multi-Proxy Reconstruction. *Astronomy and Astrophysics* 615, A93.
- Wu, Z., and Huang, N. E. (2009). Ensemble Empirical Mode Decomposition: a Noise-assisted Data Analysis Method. *Adv. Adapt. Data Anal.* 1 (1), 1–41. doi:10.1142/S1793536909000047
- Wu, L., Cai, W., Zhang, L., Nakamura, H., Timmermann, A., Joyce, T., et al. (2012). Enhanced Warming over the Global Subtropical Western Boundary Currents. *Nat. Clim. Change* 2 (3), 161–166. doi:10.1038/nclimate1353
- Wu, C.-R., Wang, Y.-L., and Chao, S.-Y. (2019). Disassociation of the Kuroshio Current with the Pacific Decadal Oscillation since 1999. *Remote Sens.* 11 (3), 276. doi:10.3390/rs11030276
- Wu, C.-R. (2013). Interannual Modulation of the Pacific Decadal Oscillation (PDO) on the Low-Latitude Western North Pacific. *Prog. Oceanogr.* 110, 49–58. doi:10.1016/j.pocan.2012.12.001
- Xiang, R., Sun, Y., Li, T., Oppo, D. W., Chen, M., and Zheng, F. (2007). Paleoenvironmental Change in the Middle Okinawa Trough since the Last Deglaciation: Evidence from the Sedimentation Rate and Planktonic Foraminiferal Record. *Palaeogeography, Palaeoclimatology, Palaeoecology* 243 (3–4), 378–393. doi:10.1016/j.palaeo.2006.08.016
- Xu, Z., Lim, D., Li, T., Kim, S., Jung, H., Wan, S., et al. (2019). REEs and Sr-Nd Isotope Variations in a 20 Ky-Sediment Core from the Middle Okinawa Trough, East China Sea: An In-Depth Provenance Analysis of Siliciclastic Components. *Mar. Geology.* 415, 105970. doi:10.1016/j.margeo.2019.105970
- Xu, D., Lu, H., Chu, G., Shen, C., Li, F., Wu, J., et al. (2020). Asynchronous 500-year Summer Monsoon Rainfall Cycles between Northeast and Central China during the Holocene. *Glob. Planet. Change* 195, 103324. doi:10.1016/j.gloplacha.2020.103324
- Yamazaki, A., Watanabe, T., Tsunogai, U., Iwase, F., and Yamano, H. (2016). A 150-year Variation of the Kuroshio Transport Inferred from Coral Nitrogen Isotope Signature. *Paleoceanography* 31 (6), 838–846. doi:10.1002/2015pa002880
- Yang, H., Lohmann, G., Wei, W., Dima, M., Ionita, M., and Liu, J. (2016). Intensification and Poleward Shift of Subtropical Western Boundary Currents in a Warming Climate. *J. Geophys. Res. Oceans* 121 (7), 4928–4945. doi:10.1002/2015JC011513
- Yang, H., Lohmann, G., Krebs-Kanzow, U., Ionita, M., Shi, X., Sidorenko, D., et al. (2020). Poleward Shift of the Major Ocean Gyres Detected in a Warming Climate. *Geophys. Res. Lett.* 47 (5), e2019GL085868. doi:10.1029/2019GL085868
- Yi, L., Yu, H.-J., Ortiz, J. D., Xu, X.-Y., Chen, S.-L., Ge, J.-Y., et al. (2012). Late Quaternary Linkage of Sedimentary Records to Three Astronomical Rhythms and the Asian Monsoon, Inferred from a Coastal Borehole in the South Bohai Sea, China. *Palaeogeography, Palaeoclimatology, Palaeoecology* 329–330, 101–117. doi:10.1016/j.palaeo.2012.02.020
- Zhao, J., Tan, L., Yang, Y., Pérez-Mejías, C., Brahim, Y. A., Lan, J., et al. (2021). New Insights towards an Integrated Understanding of NE Asian Monsoon during Mid to Late Holocene. *Quat. Sci. Rev.* 254, 106793. doi:10.1016/j.quascirev.2020.106793
- Zheng, X., Li, A., Wan, S., Jiang, F., Kao, S. J., and Johnson, C. (2014). ITCZ and ENSO Pacing on East Asian winter Monsoon Variation during the Holocene: Sedimentological Evidence from the Okinawa Trough. *J. Geophys. Res. Oceans* 119 (7), 4410–4429. doi:10.1002/2013jc009603
- Zheng, X., Li, A., Kao, S., Gong, X., Frank, M., Kuhn, G., et al. (2016). Synchronicity of Kuroshio Current and Climate System Variability since the Last Glacial Maximum. *Earth Planet. Sci. Lett.* 452, 247–257. doi:10.1016/j.epsl.2016.07.028
- Zhou, P., Shi, Z., Li, X., and Zhou, W. (2020). Response of Westerly Jet over the Northern Hemisphere to Astronomical Insolation during the Holocene. *Front. Earth Sci.* 8, 282. doi:10.3389/feart.2020.00282
- Zhu, Z., Feinberg, J. M., Xie, S., Bourne, M. D., Huang, C., Hu, C., et al. (2017). Holocene ENSO-Related Cyclic Storms Recorded by Magnetic Minerals in Speleothems of central China. *Proc. Natl. Acad. Sci. U. S. A.* 114 (5), 852–857. doi:10.1073/pnas.1610930114

Conflict of Interest: The authors declare that the research was conducted in the absence of any commercial or financial relationships that could be construed as a potential conflict of interest.

Publisher's Note: All claims expressed in this article are solely those of the authors and do not necessarily represent those of their affiliated organizations, or those of the publisher, the editors and the reviewers. Any product that may be evaluated in this article, or claim that may be made by its manufacturer, is not guaranteed or endorsed by the publisher.

Copyright © 2022 Ding, Hu, Li, Zhao, Yao, Li, Lan, Zheng and Yi. This is an open-access article distributed under the terms of the Creative Commons Attribution License (CC BY). The use, distribution or reproduction in other forums is permitted, provided the original author(s) and the copyright owner(s) are credited and that the original publication in this journal is cited, in accordance with accepted academic practice. No use, distribution or reproduction is permitted which does not comply with these terms.